

Article

# Estimation of SAR Average in Rats during 5G NR Chronic Exposure

Ramdas Makhmanazarov <sup>1,\*</sup> , Ilya Tseplyaev <sup>1</sup>, Sergey Shipilov <sup>1</sup> and Natalya Krivova <sup>2</sup>

<sup>1</sup> Radiophysics Department, National Research Tomsk State University, Tomsk 634050, Russia; narwayn@gmail.com (I.T.); s.shipilov@gmail.com (S.S.)

<sup>2</sup> Institute of Biology and Biophysics, National Research Tomsk State University, Tomsk 634050, Russia; nakri@res.tsu.ru

\* Correspondence: efemberg11@mail.ru

**Abstract:** To study physiological reactions in the brain and skin of higher mammals exposed to chronic radiofrequency radiation, specific absorption ratio (SAR) determination is required and time-consuming numerical methods are used. The paper deals with the estimation of the whole-body specific absorption rate (SAR) in rats chronically exposed to external electromagnetic fields, as well as the development of a laboratory setup simulating the operation of a fifth-generation 5G New Radio base station (with a signal bandwidth of 15 MHz and a carrier frequency of 2.4 GHz). The paper presents a modified method for theoretical SAR estimation for one-sided irradiation and distributed absorption. Mean whole-body SAR values were estimated by the proposed method and numerically modeled with the CST Microwave Studio simulation software 2020 package using primitive rat models. Dielectric parameters in the numerical simulation were used from the software library. The IEEE/IEC 62704-1 algorithm was used to investigate SAR in numerical simulations. The theoretical estimates and numerical simulations were compared for different SAR distributions and were found to be qualitatively comparable. The differences between approximate theoretical estimates and numerical simulations are 7% and 10% for distributed and non-distributed absorptions, respectively. The proposed method, which takes into account the decreasing power flux density, can be used to estimate the approximate whole-body SAR during chronic electromagnetic field exposure in rats.

**Keywords:** dosimetry; whole-body SAR; 5G NR; rats



**Citation:** Makhmanazarov, R.; Tseplyaev, I.; Shipilov, S.; Krivova, N. Estimation of SAR Average in Rats during 5G NR Chronic Exposure. *Appl. Sci.* **2024**, *14*, 208. <https://doi.org/10.3390/app14010208>

Academic Editor: Nam Kim

Received: 1 November 2023

Revised: 8 December 2023

Accepted: 18 December 2023

Published: 26 December 2023



**Copyright:** © 2023 by the authors. Licensee MDPI, Basel, Switzerland. This article is an open access article distributed under the terms and conditions of the Creative Commons Attribution (CC BY) license (<https://creativecommons.org/licenses/by/4.0/>).

## 1. Introduction

With the rapid evolution of modern technologies, a frequency range from 100 MHz to 300 GHz is firmly in place to run various devices. Sources of radiation are household appliances, medical and industrial equipment, and radio communications. The impact of electromagnetic (EM) waves has become an integral part of our lives. A question as to whether they have a negative effect on the human body has prevailed over a long time and attracts a lot of research [1]. With the massive deployment of advanced wireless networks, the number of users constantly rises. The 5G NR standard supporting Internet of Things applications will massively increase a number of users, and, consequently, the level of the electromagnetic field (EMF) in human life. The effect caused by electromagnetic exposure on living things is relevant in many studies today.

The biological effects of EMFs are evaluated in laboratory studies involving animals, phantoms of biological tissues, and cell cultures. The interaction of EM energy with biological tissues (in the physical sense) seems to be a complex and unsafe process for a living thing. Due to these interactions, magnetic fields are distributed unevenly in rats and local currents are induced, regardless of the external E-field being uniform or not. Local fields and currents are connected in a complex way with incident external electromagnetic fields, as well as the geometric and physical parameters of rats. The interaction implies the

absorption of incident EM energy and the distribution of the absorbed exposure energy in rats.

To date, there are several international documents on recommendations for limiting both short-term and long-term, continuous and intermittent radio frequency (RF) EM exposures. These recommendations are based on thorough scientific assessments. The main sources of such documents are the International Commission on Non-Ionizing Radiation Protection (ICNIRP) and the Institute of Electrical and Electronics Engineers (IEEE) [1–3].

The key values used as quantitative limits on the EMF effects on a person are the power density and the specific absorption rate (SAR). SAR characterizes the amount of electromagnetic energy absorbed per unit mass. Pursuant to ICNIRP and IEEE documents, a value to be used depends on EMF frequencies and exposure subjects. The Russian Federation establishes sanitary rules and regulations estimating the maximum permissible EMF values by the power density in the frequency range from 300 MHz to 300 GHz [4]. Thus, determination of these values is important when conducting studies of EMF effects on living organisms or their phantoms.

Depending on the conditions of experiments with animals and the irradiation procedure, SAR estimation can be performed in different ways. Even before the coming of 5G technologies, there are many known studies related to SAR estimation. There are many studies on the development of single anechoic chambers [5]. The authors paid attention to the influence of the field inhomogeneity obtained in the presence of the cell, which was found to be not significant in the SAR estimation. SAR was determined using calorimetric and thermographic methods. The authors of [6,7] developed the Radial Electromagnetic Cavity, which is optimized for irradiation of the whole body of mice *in vivo* with 900 MHz radiofrequency fields. In [8], an exposure setup with up to 30 rats at the bottom of an anechoic chamber was utilized. 900 MHz plane-wave microwaves were emitted from a horn antenna located 600 mm above the animals. All animals were located individually in plastic cages small enough to align them in the direction of the long axis parallel to the electric field. SAR was estimated on gel-based phantoms using a temperature change measurement technique.

A notable work, in terms of the radiating setup, is presented in the study [9]. The authors exposed 100 mice to a modulated 900 MHz field. A quarterwave monopole inside a room covered with aluminum was used as the source. Twenty animal cages, each containing five unrestrained animals oriented parallel to the long axis of the antenna, were mounted on the wall perpendicular to the ground plane in a circular array at a radius of 650 mm around the antenna. The room was reflective, resulting in an undefined standing wave pattern, and the animals were allowed to move freely in the cage as well as to converge. In the cages' area, the incident power density values varied from 2.6 to 13 W/m<sup>2</sup>. The whole-body SAR estimations were provided by measuring the internal EMF components of the mice phantom per 1 W/m<sup>2</sup>, which were then recalculated to the actual power density. Measurements of the EMF fields induced by RF fields were made on three phantoms representing small, medium, and large mice in a semi-anechoic room.

In [10,11], the authors present the design features and technical implementation of radiofrequency irradiation systems developed for the National Toxicology Program (NTP). The reverberation chambers were characterized in terms of the homogeneity of the electromagnetic field inside the chambers. SAR was evaluated using the thermometric method on phantoms.

More recent studies related to fifth-generation cellular technologies are also known. The range of available frequencies for the implementation of 5G NR modulation, which is defined in Tables 5.2-1 and 5.2-2 of 3GPP TS38.104 [12], varies from 410 MHz to 7125 MHz (FR1) and 24,250 MHz to 52,600 MHz (FR2). Different frequencies are used in different regions.

In [13,14], the effect of 5G signals with a frequency of 3.5 GHz on living human cells' keratinocytes and fibroblasts was investigated. The SAR was assessed by the thermometric method [14]. In study [15], the authors investigated the effects of 4.9 GHz (one of the work-

ing frequencies of 5G communication) radiofrequency (RF) field on emotional behaviors and spatial memory in adult male mice. Mice were exposed to 4.9 GHz radiofrequency radiation for 21 days, at 1 h/day. The power density (PD) was  $50 \text{ W/m}^2$  and the distance from the radiation antenna to the target animals was 70 cm. SAR measurements were not provided. A wide review was presented in [16] for frequencies 6–100 GHz. The authors analyzed 94 relevant publications performing *in vivo* or *in vitro* investigations.

In addition to biological studies, various techniques for SAR estimation are being developed, in particular using numerical methods [17–19]. In [19], the authors adopted the Poggio–Miller–Chang–Harrington–Wu–Tsai formulation of the method of moments to directly determine the specific absorption rate (SAR) of differently shaped dielectric phantoms placed in an RC and demonstrated its validity via comparing the numerical temperature rise with those obtained from experiments. Resonant absorption studies, based on the antenna theory [20,21], are also known.

Analyzing approaches to animal experimentation from the available literature, it can be seen that they may be conceptually different. Obviously, one or another experimental design is justified by the researchers. Based on the overall concept of the experiment and the available resources, a certain methodology is used. This paper considers the problem of SAR estimation in an experiment [22], which conceptually differs significantly from the majority of works. For long-term experiments to study the physiological reactions of animals, 24 h irradiation of free-behaving animals in natural laboratory conditions is required. In other words, animals need to be kept with minimal interference in their “domestic” life to eliminate stress factors. A similar concept was in study [9]. Under such conditions, an objective estimate of the SAR can be quantified at the maximum and minimum limits. It is also necessary to set exposure regimes to avoid increasing the temperature of exposed animals and to ensure safe levels for laboratory personnel.

Taking into account the mentioned requirements, in the Section 2, we present a description of the radiating setup in the experiment [22], the components used and their characteristics, as well as its operation modes. In the following, the derivation of the formula for theoretical SAR estimation, which takes into account the decreasing power flux density, is given. Further in the numerical simulation section, the information of the simulation parameters is outlined. The Section 3 presents the SAR values for different exposure options obtained in the simulation and from the theoretical formula. And finally, a discussion and conclusion of the results obtained are given at the end, Sections 4 and 5.

## 2. Materials and Methods

### 2.1. Experimental Procedure

The Adalm pluto SDR (software-defined radio) active learning module is used as a source for generating 5G NR signals. A downlink frequency range signal FR1 was used—from a base station to a user. The signal was produced using a software package for generating test signals of the 5G NR standard, developed under agreement No. 075-11-2019-031 with the Ministry of Science and Higher Education of the Russian Federation, dated 26 November 2019. The bandwidth of the generated signal is 15 MHz and the carrier frequency is 2.4 GHz. The signal spectrum is shown in Figure 1.

The 2.4 GHz frequency is chosen for several reasons. First, this frequency is defined in Table 5.2-1 of 3GPP TS38.104 [12]. Secondly, the ratio of the wavelength at this frequency to the animal length is different from 1, which avoids the possible temperature rise caused by the resonant absorption described in [21,23,24]. In the third, this range is already widely used in WiFi technologies, which allows us to generalize the research to some extent. Also, this band has performed well in terms of coverage distance, compared to higher frequencies.

To amplify the signal, a blm9D2324-25b amplifying module was used with a gain of 28 dB in a given frequency range. A PlastRam antenna, developed at TSU Department of Radiophysics, was used as a radiating unit with dimensions  $240 \times 168 \text{ mm}$ . The combined

linear polarization antenna has one feed port with an impedance of 50 Ohm and is an electric and magnetic dipole with a combined phase center.

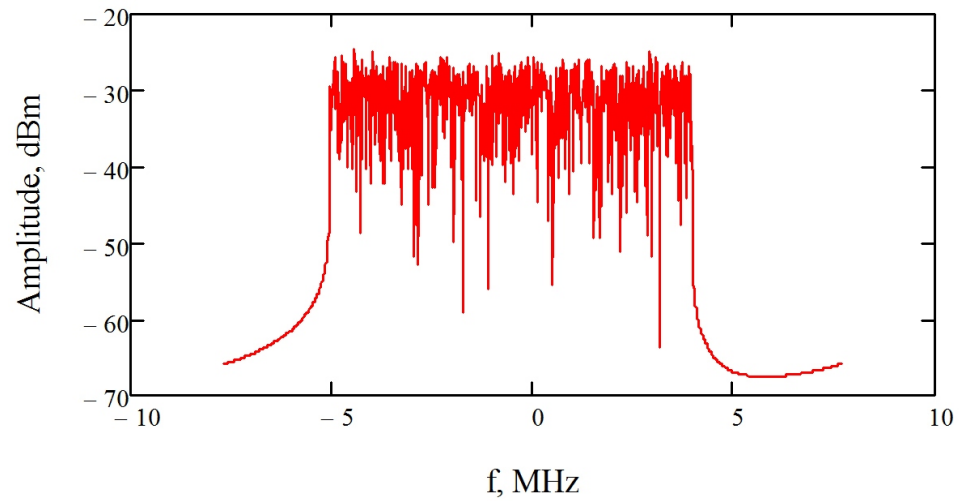


Figure 1. Zero-frequency Signal Spectrum.

Figure 2 shows the radiation pattern (RP) of the antenna at a frequency of 2.4 GHz. The RP has two symmetrical lobes, which enables uniform whole-body exposures of two rats. The antenna gain is 7 dBi. For the combined antenna applied, electrical and magnetic energy are considered to become balanced at distances longer than a wavelength (12.5 cm).

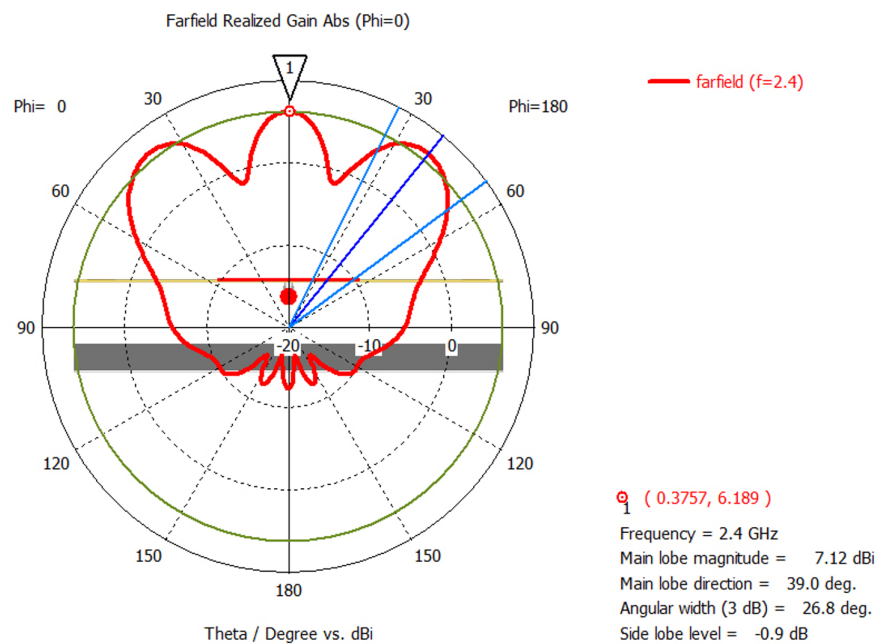
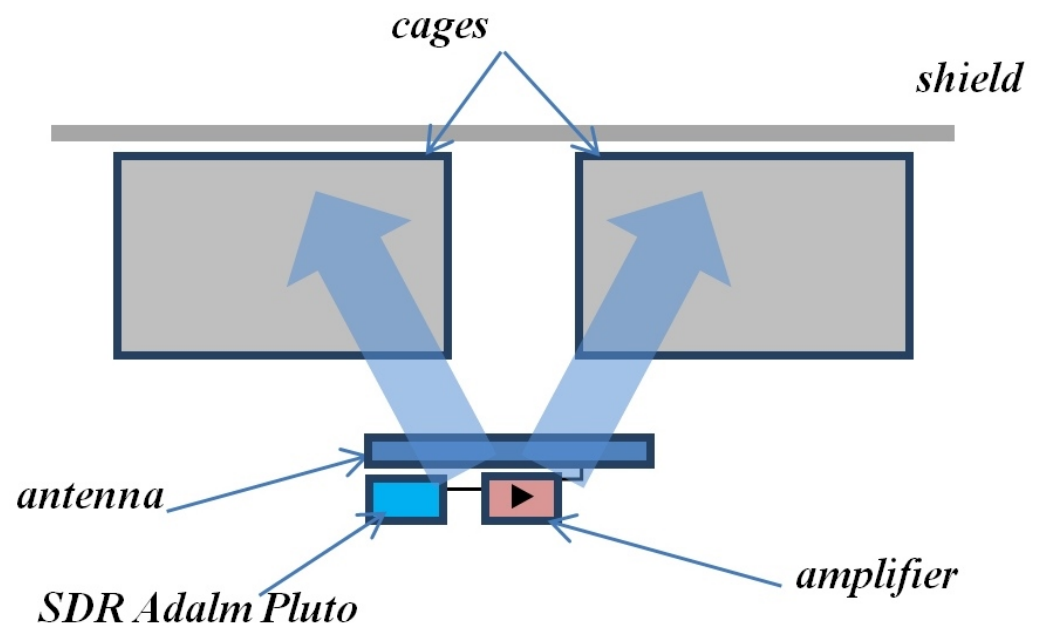


Figure 2. Free Antenna Pattern and characteristics [1].

Figure 3 shows a schematic for an experimental setup designed to study the exposure effects of a 5G NR base station. A radiating unit consisting of a network device, a cascade amplifier, and an antenna is powered from an external source and exposes the cages (Techniplast) from one side. A shield (with dimensions of 98 × 25 cm) is placed on the other side, to limit any possible exposure from the outside.



**Figure 3.** Experimental design.

The signal power supplied to the antenna was 0.5 W and 0.0891 W for various exposure cases. The choice of these levels is related to ensuring that the SAR does not exceed the ICNIRP restrictions for whole-body SAR. The power was measured with an M3M-18 microwave power meter (Micran).

All animals were treated in accordance with the EU Council Directive of 24 November 1986 (86/609/EEC) and were approved by the Animal Research Ethics Committee of Tomsk State University.

Three dose groups of male Wistar rats were used in experiment. The first and second groups of experimental animals included 10 rats (5 per cage) with an average weight of 488 g and a length of 25 cm. The first group was exposed to 24 h radiation for a week with an average dose of 3.393 W/m<sup>2</sup>. The antenna was placed 12 cm away from the cages.

The second group was exposed to 24 h EMF radiation for 4 weeks with a dose of 0.605 W/m<sup>2</sup>. The third group included 20 young rats (10 per cage) with an average weight of 295 g and a length of 20 cm. The antenna was placed 20 cm away from the cages. To equalize the average SAR, the third group was exposed to a lower average dose (0.31 W/m<sup>2</sup>).

Figure 4 shows that the rats could roam freely within their individual cages, thereby receiving different electromagnetic doses. In this exposure configuration, the absorption in the cage becomes spatially distributed.



**Figure 4.** Laboratory setups.

## 2.2. Dosimetry Study

The whole-body average SAR values (exposure volume) are 0.08 W/kg for the general public and 0.4 W/kg for RF EMF workers, regardless of the frequency of radiation [2,25]. The SAR value is determined as follows:

$$SAR = \frac{d}{dt} \left( \frac{dW}{dm} \right) = \frac{\sigma |E|^2}{\rho} \left[ \frac{W}{kg} \right], \quad (1)$$

where  $m$ ,  $t$ , and  $W$  are mass [kg], time [s], and energy [J] of the EMF, respectively.  $\sigma$  is the specific electrical conductivity of a biological tissue in [S/m],  $E$  is the E-field strength in a matter [V/m], and  $\rho$  is the density of a matter [kg/m<sup>3</sup>] [3,25].

There are several experimental methods for determining SAR, including waveguide methods, calorimetric and thermometric methods, as well as methods based on measuring the EMF components in biomaterials [3,26]. The methods are not always applicable, as they require special instruments and have certain restrictions when dosimetry is applied to measure radiation absorbed by living things. Therefore, in a real-life setting, it is not always feasible to accurately determine SARs.

There are many publications [20,21,24,27,28] on the qualitative assessment of SAR for biological subjects. The studies investigated the frequency dependence of SAR with geometric dimensions of objects, as well as when exposed to different polarizations of radiation.

In [24], the expressions are given for assessing the whole-body average SAR at the EMF free-space power density  $S_{inc}$ , for different ratios  $L/\lambda$ , where  $L$ ,  $\lambda$  are the lengths of the body and the wave, respectively. In particular, for  $L/\lambda > 0.4$ :

$$SAR_{avg} = \frac{5.954}{f_{GHz}} \frac{S_{inc} L}{m} \left[ \frac{W}{kg} \right], \quad (2)$$

where  $m$  is the mass of the animal in kilograms,  $L$  is in meters, and  $S_{inc}$  is in W/m<sup>2</sup> [24]. It has been shown that expression (2) describes well the distribution of SAR from the frequency when the object is oriented parallel to the E-polarization. In the limit, expression (2) tends to the "optical" description of absorption ( $1 - Refl$ ).

In vivo determination of SARs for a group of rats kept in a normal cage was rendered complex due to many impacts. During the prolonged and one-sided EMF exposure in the cage, the rats were located in different proximities from the antenna and were free to move randomly. In addition, the weight of the rats changed during the experiment. All of the above factors contributed to an accurate SAR estimate.

Given the above, a rough estimate of the SAR can be expressed as:

$$SAR_{avg} = \frac{5.954}{f_{GHz}} \frac{\langle S_{inc} \rangle \langle L \rangle}{\langle m \rangle}, \quad (3)$$

where  $S_{inc}(r) = P_A G / 4\pi r^2$ ,  $P_A$  is the power supplied to the antenna [W],  $G$  is the antenna gain [dB],  $r$  is the distance from the antenna [m], and  $\langle \rangle$  is the averaging.

## 2.3. Numerical Simulations

To evaluate the SAR under the approximated experimental conditions presented in Figure 3, numerical simulations of the experiment were carried out for 2 and 10 rats (Figure 4) in the CST Microwave Studio software package. A primitive 3d rat model was used from [29] as a rat phantom, with the dielectric parameters of blood ( $\epsilon' = 58.34$  and  $\epsilon'' = 18.76$ ).

The rat phantom was 16 cm long and weighed 180 g. In the real world, a rat is a heterogeneous body, which is composed of many types of tissues. We believe that it is sufficient to use a homogeneous dielectric model instead of an heterogeneous one for qualitative evaluation. In addition, the characteristics of the simplified phantoms, in terms of body mass to the maximum length ratio, are close to the ratio of the experimental animals.

The cage size was set to  $480 \times 375 \times 210$  mm, with a wall thickness of 10 mm ( $\epsilon = 3$  and  $tg(\epsilon''/\epsilon') = 0.001$ , polycarbonate). On top, the case was closed with a metal lid (cage top equivalent) and a metal shielding on the back side. The distance of the shielding to the nearest phantom is 2 cm. The shortest distance from the antenna to the shielding is 43 cm.

The EMF was calculated using the default finite integration method in the time domain of the CST microwave studio package. The algorithm IEEE/IEC 62704-1 was used to calculate SARs. This is an accepted averaging method according to IEC/IEEE 62704-1:2017 on “Determination of Peak Spatial Averaged Specific Absorption Rate (SAR) in the Human Body from Wireless Communication Devices, 30 MHz to 6 GHz—Part 1: General Requirements for Use of Finite-Difference Time Domain Method (FDTD) for SAR Calculations” [2,3,25].

The mesh partitioning in the case for 10 rats was 226,735,740 cells and for two rats was 65,486,652 cells. All calculations were performed on AMD Ryzen 7 3800X (8-core) 3.89 GHz CPU and NVIDIA GeForce RTX3060 GPU.

When the cages were located in front of the antenna (Figure 5), its VSWR did not exceed 1.8 in the operating frequency range (Figure 6). The values of the dielectric parameters for the frequency of 2.4 GHz were also used from the tables of the software package, which were consistent with the ones generally accepted.

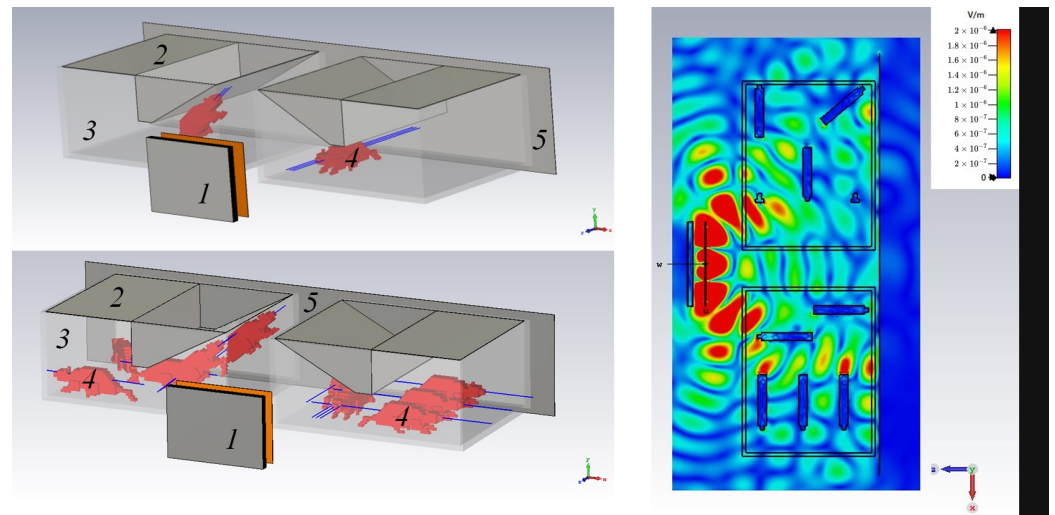


**Figure 5.** Experiment Simulations for SAR Calculations (left). 1—antenna, 2—metal lid, 3—cage body, 4—rat phantom, and 5—metal shield. Field Distribution in the OXZ Plane (right).

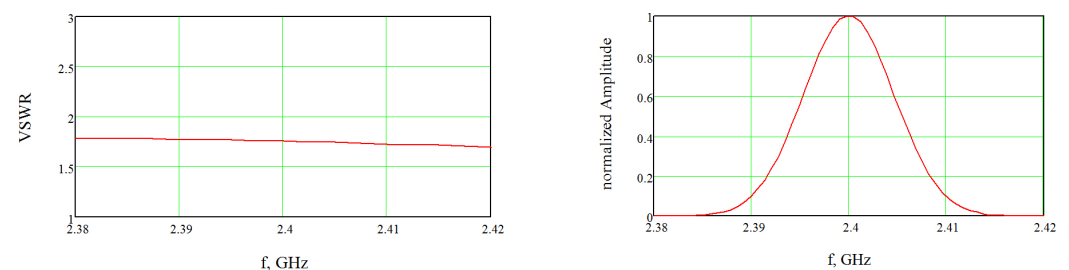


**Figure 6.** Standing-wave Ratio and Normalized spectrum of signal applied to the Antenna in Numerical Simulations.

### 3. Results

Numerical and experimental findings suggest that the average SAR value for two rats was 0.202 W/kg and for 10 rats was 0.0818 W/kg, with the distance between the antenna and the nearest phantom being 20 cm.

The whole-body average SARs decreased by several times as the number of rats in the cage increased. This depended on different positions of the rats in the cage relative to the

antenna. Similar calculations were proposed for  $P_A = 0.2$  W. The results are presented in Table 1.

**Table 1.** SAR numerical simulations and theoretical estimates.

Group Type	$P_A$ [W]	$S_{inc}$ [W/m <sup>2</sup> ]	$SAR_{avg}$ [W/kg]
Non-distributed absorption	1	10.25	0.202 (model) 0.226 (theory)
Non-distributed absorption	0.2	2.05	0.0404 (model) 0.0452 (theory)
Distributed absorption	1	3.474	0.0818 (model) 0.0766 (theory)
Distributed absorption	0.2	0.695	0.0163 (model) 0.0153 (theory)

The numerical simulation results in Table 1 are obtained via a once-through calculation of the model. To compare the results, we enter the percentage difference  $D$  between numerical simulations and theoretical estimates:

$$D = \left(1 - \frac{\min(n, t)}{\max(n, t)}\right) \times 100\%, \quad (4)$$

where  $n$  and  $t$  are numerical simulations and theoretical estimates, respectively. For the non-distributed absorption,  $D$  7%, and for the distributed absorption,  $D$  10%. For the case of non-distributed absorption within the cage, i.e., for the case with two rats, theoretical estimates can be made by expression (2) for  $S_{inc} = 10.25$  W/m<sup>2</sup>, of which the average SAR is 0.226 W/kg. For the case of distributed absorption (10 rats), the average SAR theoretical estimate by expression (3) is 0.0766 W/kg. For in vivo experiment theoretical estimates of SARs, they are presented in Table 2 and Figure 7.

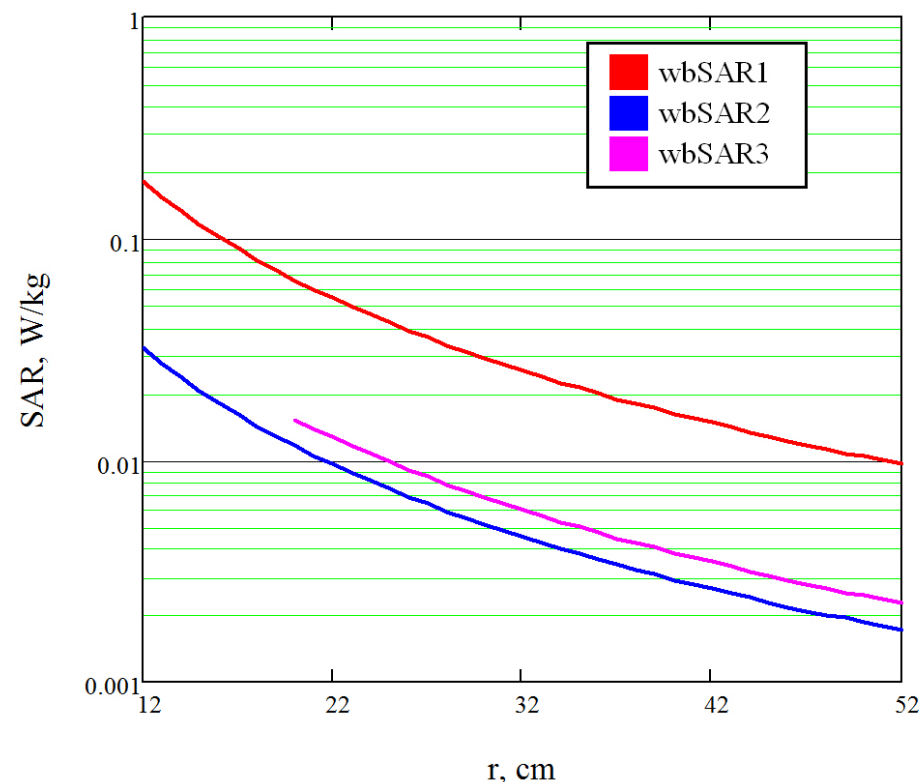


**Figure 7.** Theoretical Estimation of SAR Distributions for Experimental Groups.

**Table 2.** Theoretical SAR Estimation for Experimental Groups.

Group Type	$P_A$ [W]	$\langle S_{inc} \rangle$ [W/m <sup>2</sup> ]	$SAR_{avg}$ [W/kg]
wbSAR1	0.5	3.393	0.180 (max) 0.0431 (mean) 0.009 (min)
wbSAR2	0.0891	0.605	0.0322 (max) 0.0076 (mean) 0.0017 (min)
wbSAR3	0.0891	0.31	0.0153 (max) 0.0059 (mean) 0.0022 (min)

#### 4. Discussion

Table 1 shows a discrepancy between theoretical estimates and numerical simulations in the case of non-distributed absorption. This discrepancy may be due to several reasons. Firstly, since expression 1.1 was empirically derived for the case of free space exposure, it did not take into account re-reflections [24]. Secondly, the posture positions of animals in the space relative to the polarization of the exposure affected the final absorption; however, it was also noted in [24,30] that for  $L/\lambda \gg 0.4$ , the effect of the polarization orientation relative to the object on the SAR is small. Due to the complex geometry of the reflectors in the exposure environment, “nulls” and interference extrema can be formed, which also affect the absorption [19–21,24,27,28]. Depending on the positions of the phantom in such “hot” or “null” spots, the exposure will increase or decrease, respectively. In the case of distributed absorption, the exposure increased in the model, which was expected due to re-reflections and a higher probability of entering into “hot” interference spots. In the numerical modeling, the effect of re-reflection is taken into account and we believe that the difference of 7–10% compared to the theoretical estimate is due to this phenomenon. We do not exclude that re-reflections may contribute more to the SAR, in the case of the increasing exposure power density. However, at a comparatively lower power, assuming the exposure decreases as  $1/r^2$ , the effects of re-reflection will contribute even less. The development of a generalized SAR estimation technique taking into account the influence of re-reflections requires additional studies based on the statistical analysis of the distribution of elements, animals, and configurations of electromagnetic fields. Studies in this direction are described in [19,30,31] and they are still in progress. Great successes have been achieved mainly for the case of completely closed reverberation or anechoic chambers.

The paper [30] presents the results of the numerical calculation of SAR for the anatomical model of the Sprague–Dawley rat with 31 tissues in the frequency range of 0.5–5 GHz at EMF power density  $S_{inc} = 1$  W/m<sup>2</sup>. High-resolution models are mainly important for the study of local volume SAR, and the authors presented both local and whole-body SAR. The whole-body SAR is composed of such local absorptions, where we believe that it is sufficient to use a homogeneous dielectric model instead of a heterogeneous one for qualitative evaluation. At GHz frequencies, waves penetrate less deeply and are reflected more. This is due to the increased conductivity of the skin tissue layer at these frequencies [32,33]. Conductivity in tissues is in turn related to blood and other substances with high conductivity. Since blood is present in almost the entire volume of the animal, we used a rat phantom with the dielectric parameters of blood. We agree that this approach does not provide true SAR values, but we can compare estimates regarding distributed and non-distributed absorption.

A comparison can be made using the example of an estimate for a rat model with  $L = 24.4$  cm and  $m = 220$  g at 2.4 GHz, where whole-body SAR is 0.027 W/kg [30]. This value agrees perfectly with the estimate from expression (1). It is difficult to compare the estimates for the distributed absorption since we know only one work with the concept of radiation with a decreasing incident power density of a group of animals [9]. The

study presents SAR values ranging from 0.13 for H-polarization to 1.4 W/kg in the E-polarization plane. Using the description from [9], we estimated the distributed absorption using expression (3), taking into account the decreasing incident power density within the cage. Assuming an average mouse size of 10 cm (since this information was missing from the description), we obtained a maximum of 1.387 W/kg, a minimum of 0.663 W/kg, and a mean of 0.951 W/kg for E-polarization. An estimation of SAR, taking into account H-polarization in this case, is not possible because the used frequency does not satisfy the condition  $L/\lambda \gg 0.4$ . For E-polarization, the upper bound of the SAR is close to the presented [9] authors, while the lower value was not presented. Thus, it can be concluded from the obtained results that the proposed expression (3) can be used for approximate SAR estimation in the case of distributed absorption, taking into account the decreasing incident power density. The SAR estimates presented in Figure 7 were necessary to establish exposure regimes so as not to exceed the basic ICNIRP limits for whole-body SAR.

## 5. Conclusions

Despite the rough approximations of rat phantoms used in simulations, the numerical calculation of SAR is qualitatively comparable to the theoretical estimate. A more accurate estimate requires the use of high-resolution model phantoms and a more detailed statistical analysis of EMF distribution and animal position. The differences between the approximate theoretical estimate and numerical simulations were 7% and 10% for the distributed and non-distributed absorptions, respectively. The whole-body average SARs in the approximate in vivo theoretical estimates were 0.0431, 0.0076, and 0.0059 W/kg for the first, second, and third groups, respectively.

In fact, ambient illumination in combination with multiple reflections make accurate dosimetry more challenging. Adjustments to the actual amount of absorbed power are made by the fact that a living thing cannot stand still in a long-term experiment.

The waveguide method can be considered the most accurate measurement of the whole body average SAR. It is possible to measure the power transmitted and reflected from the subject, which can accurately determine the specific absorption rate. However, such conditions are not suitable for long-term experiments to study the physiological reactions of animals.

In [2], a threshold value of 4 W/kg under various exposure conditions was believed to cause some animal species, including non-human primates, to alter their complex behavioral patterns. Behavioral disturbance is often (but not always) accompanied by a 1.0 °C rise in body temperature. Even at exposure levels well above current standards, human body temperature is effectively regulated by mobilizing appropriate heat loss mechanisms such as sweating and skin blood flow.

All first-group study animals (SAR = 0.043 W/kg) were recorded to have their body temperature rise by an average of 1 °C. In addition, the maximum possible absorption exceeded the allowable norms by  $0.18/0.08 = 2.25$  times. Despite the fact that the average SAR value was below the acceptable level, prolonged EMF exposure caused a rise in temperature. Changing temperatures were not registered during the exposure of rats. The study of physiological reactions of animals in the first group was stopped because the temperature increase was not acceptable. The other groups were within normal temperature limits, and the results of physiologic studies are described in [22]. Expression (3) requires modifications related to the statistical distribution of the positions of rats in the cage. The posture positions of rats obviously depend on their number in the cage, the shape of the cage, the location of the feeder, the behavioral properties of the animals, etc. The developments in this domain are being planned for the near future.

**Author Contributions:** Conceptualization, N.K. and S.S.; methodology, R.M., N.K., and S.S.; software, I.T. and R.M.; validation, R.M., I.T., and S.S.; formal analysis, R.M. and S.S.; investigation, R.M.; resources, N.K. and S.S.; data curation, N.K. and S.S.; writing—original draft preparation, R.M.; writing—review and editing, S.S., I.T., and N.K.; visualization, R.M. and I.T.; supervision, S.S.; project

administration, N.K.; funding acquisition, N.K. All authors have read and agreed to the published version of the manuscript.

**Funding:** This research was funded by Tomsk State University Development Programme (Priority-2030) grant number NU 2.4.9.22 ONG—“The Study of Physiological Reactions in the Brain and Skin of Higher Mammals Exposed to Chronic RF 5G Radiation”.

**Institutional Review Board Statement:** All animals were treated in accordance with the EU Council Directive of 24 November 1986 (86/609/EEC) and were approved by the Animal Research Ethics Committee of Tomsk State University.

**Informed Consent Statement:** Not applicable.

**Data Availability Statement:** The data used to support the findings of this study are included within the article.

**Conflicts of Interest:** The authors declare no conflicts of interest.

## Abbreviations

The following abbreviations are used in this manuscript:

SAR	Specific absorption rate
5G NR	5 Generation New Radio
EM	Electromagnetic
RF	Radio frequency
ICNIRP	International Commission on Non-Ionizing Radiation Protection
IEEE	Institute of Electrical and Electronics Engineers
SDR	Software-defined radio
RP	Radiation pattern
EMF	Electromagnetic field
FDTD	Finite-Difference Time Domain
VSWR	Voltage standing wave ratio

## References

- World Health Organization. *Electromagnetic Fields and Public Health: Mobile Phones*. 2014. Available online: <https://www.who.int/ru/news-room/fact-sheets/detail/electromagnetic-fields-and-public-health-mobile-phones> (accessed on 6 June 2021).
- ICNIRP. Guidelines for limiting exposure to electromagnetic fields (100 kHz to 300 GHz). *Health Phys.* **2020**, *118*, 483–524. [[CrossRef](#)] [[PubMed](#)]
- IEEE. IEEE Recommended Practice for Measurements and Computations of Radio Frequency Electromagnetic Fields With Respect to Human Exposure to Such Fields, 100 kHz–300 GHz. IEEE Std C95.3-2002 (Revision of IEEE Std C95.3-1991) 2002, i–126. Available online: <https://ieeexplore.ieee.org/servlet/opac?punumber=8351> (accessed on 6 June 2021).
- Goskomepidnadzor, 1996. *RADIOFREQUENCY ELECTROMAGNETIC RADIATION (RF EMR) Under occupational and conditions. Federal Sanitary Rules, Norms and Hygiene Standards SANPIN 2.2.4/2.1.8.055-96*. Available online: <https://files.stroyinf.ru/Data2/1/4294851/4294851561.pdf> (accessed on 6 June 2021).
- Guy, A. Miniature anechoic chamber for chronic exposure of small animals to plane-wave microwave fields\*. *J. Microw. Power* **1979**, *14*, 327–338. [[CrossRef](#)] [[PubMed](#)]
- Balzano, Q.; Chou, C.; Cicchetti, R.; Faraone, A.; Tay, R.S. An efficient RF exposure system with precise whole-body average SAR determination for in vivo animal studies at 900 MHz. *IEEE Trans. Microw. Theory Tech.* **2000**, *48*, 2040–2049. [[CrossRef](#)]
- Hansen, V.; Bitz, A.; Streckert, J. RF exposure of biological systems in radial waveguides. *IEEE Trans. Electromagn. Compat.* **1999**, *41*, 487–493. [[CrossRef](#)]
- Chagnaud, J.L.; Veyret, B. Rapid communication: In vivo exposure of rats to GSM-modulated microwaves: Flow cytometry analysis of lymphocyte subpopulations and of mitogen stimulation. *Int. J. Radiat. Biol.* **1999**, *75*, 111–113. [[CrossRef](#)] [[PubMed](#)]
- Repacholi, M.H.; Basten, A.; Gebiski, V.; Noonan, D.; Finnie, J.; Harris, A.W. Lymphomas in Eμ-Pim1 Transgenic Mice Exposed to Pulsed 900 MHz Electromagnetic Fields. *Radiat. Res.* **1997**, *147*, 631–640. [[CrossRef](#)] [[PubMed](#)]
- Capstick, M.H.; Kuehn, S.; Berdinas-Torres, V.; Gong, Y.; Wilson, P.F.; Ladbury, J.M.; Koepke, G.; McCormick, D.L.; Gauger, J.; Melnick, R.L.; et al. A Radio Frequency Radiation Exposure System for Rodents Based on Reverberation Chambers. *IEEE Trans. Electromagn. Compat.* **2017**, *59*, 1041–1052. [[CrossRef](#)]
- Gong, Y.; Capstick, M.; Kühn, S.; Wilson, P.; Ladbury, J.; Koepke, G.; McCormick, D.; Melnick, R.; Kuster, N. Life-Time Dosimetric Assessment for Mice and Rats Exposed in Reverberation Chambers for the Two-Year NTP Cancer Bioassay Study on Cell Phone Radiation. *IEEE Trans. Electromagn. Compat.* **2017**, *59*, 1798–1808. [[CrossRef](#)]

12. 3GPP. 5G; NR; Base Station (BS) Radio Transmission and Reception (Release 16). Technical Specification (TS) 38.104, 3rd Generation Partnership Project (3GPP), 2020. Version 16.4.0. Available online: [https://www.etsi.org/deliver/etsi\\_ts/138100\\_138199/138104/16.04.00\\_60/](https://www.etsi.org/deliver/etsi_ts/138100_138199/138104/16.04.00_60/) (accessed on 6 June 2021).
13. Joushomme, A.; Orlacchio, R.; Patrignoni, L.; Canovi, A.; Chappe, Y.; Poullietier de Gannes, F.; Hurtier, A.; Garenne, A.; Lagroye, I.; Moisan, F.; et al. Effects of 5G-modulated 3.5 GHz radiofrequency field exposures on HSF1, RAS, ERK, and PML activation in live fibroblasts and keratinocytes cells. *Sci. Rep.* **2023**, *13*, 8305. [\[CrossRef\]](#)
14. Orlacchio, R.; Andrieu, G.; Joushomme, A.; Patrignoni, L.; Hurtier, A.; de Gannes, F.P.; Lagroye, I.; Percherancier, Y.; Arnaud-Cormos, D.; Lévêque, P. A Novel Reverberation Chamber for In Vitro Bioelectromagnetic Experiments at 3.5 GHz. *IEEE Trans. Electromagn. Compat.* **2022**, *65*, 39–50. [\[CrossRef\]](#)
15. Qin, T.Z.; Wang, X.; Du, J.Z.; Lin, J.J.; Xue, Y.Z.; Guo, L.; Lai, P.P.; Jing, Y.T.; Zhang, Z.W.; Ding, G.R. Effects of radiofrequency field from 5G communications on the spatial memory and emotionality in mice. *Int. J. Environ. Health Res.* **2022**, *11*, 1–12. [\[CrossRef\]](#) [\[PubMed\]](#)
16. Simkó, M.; Mattsson, M.O. 5G Wireless Communication and Health Effects—A Pragmatic Review Based on Available Studies Regarding 6 to 100 GHz. *Int. J. Environ. Res. Public Health* **2019**, *16*, 3406. [\[CrossRef\]](#) [\[PubMed\]](#)
17. Findlay, R.P.; Lee, A.K.; Dimbylow, P.J. FDTD calculations of SAR for child voxel models in different postures between 10 MHz and 3 GHz. *Radiat. Prot. Dosim.* **2009**, *135*, 226–231. [\[CrossRef\]](#) [\[PubMed\]](#)
18. Chakarothai, J.; Wang, J.; Fujiwara, O.; Wake, K.; Watanabe, S. A Hybrid MoM/FDTD Method for Dosimetry of Small Animal in Reverberation Chamber. *IEEE Trans. Electromagn. Compat.* **2014**, *56*, 549–558. [\[CrossRef\]](#)
19. Chakarothai, J.; Wang, J.; Fujiwara, O.; Wake, K.; Watanabe, S. Dosimetry of a Reverberation Chamber for Whole-Body Exposure of Small Animals. *IEEE Trans. Microw. Theory Tech.* **2013**, *61*, 3435–3445. [\[CrossRef\]](#)
20. Hirata, A.; Fujiwara, O.; Nagaoka, T.; Watanabe, S. Estimation of Whole-Body Average SAR in Human Models Due to Plane-Wave Exposure at Resonance Frequency. *IEEE Trans. Electromagn. Compat.* **2010**, *52*, 41–48. [\[CrossRef\]](#)
21. Hirata, A.; Yanase, K.; Laakso, I.; Hung, K.; Fujiwara, O.; Nagaoka, T.; Watanabe, S.; Conil, E.; Wiart, J. Estimation of the whole-body averaged SAR of grounded human models for plane wave exposure at respective resonance frequencies. *Phys. Med. Biol.* **2012**, *57*, 8427–8442. [\[CrossRef\]](#)
22. Krivova, N.; Kudabaeva, M.; Zayeva, O.; Borodina, S.; Lepyokhina, T.; Borodina, S.; Makhmanazarov, R.; Kokin, D.; Shipilov, S. The Effect of Chronic Exposure to 5G Radio Frequency Radiation on the Body in Male Wistar Rats of Different Ages. Manuscript under review in Scientific Reports.
23. Hirata, A.; Sugiyama, H.; Fujiwara, O. Estimation of core temperature elevation in humans and animals for whole-body averaged SAR. *Prog. Electromagn. Res.* **2009**, *99*, 221–237. [\[CrossRef\]](#)
24. Gandhi, O.P.; Hunt, E.L.; D’Andrea, J.A. Deposition of electromagnetic energy in animals and in models of man with and without grounding and reflector effects. *Radio Sci.* **1977**, *12*, 39–47. [\[CrossRef\]](#)
25. Bailey, W.H.; Bodemann, R.; Bushberg, J.; Chou, C.K.; Cleveland, R.; Faraone, A.; Foster, K.R.; Gettman, K.E.; Graf, K.; Harrington, T.; et al. Synopsis of IEEE Std C95.1™-2019 “IEEE Standard for Safety Levels With Respect to Human Exposure to Electric, Magnetic, and Electromagnetic Fields, 0 Hz to 300 GHz”. *IEEE Access* **2019**, *7*, 171346–171356. [\[CrossRef\]](#)
26. Kudryashov, Y. (Ed.) *Radiatsionnaya Biofizika: Radiochastotniye, Mikrovolnoviye Elektromagnitniye Izlucheniya (Radiation Biophysics: Radio Frequency and Microwave Electromagnetic Radiation)*; FIZMATLIT: Moscow, Russia, 2008.
27. Gandhi, O.; Riazi, A. Absorption of Millimeter Waves by Human Beings and its Biological Implications. *IEEE Trans. Microw. Theory Tech.* **1986**, *34*, 228–235. [\[CrossRef\]](#)
28. Gandhi, O. State of the knowledge for electromagnetic absorbed dose in man and animals. *Proc. IEEE* **1980**, *68*, 24–32. [\[CrossRef\]](#)
29. pála vedcom. Voxel Rat on His Tail. 2019. Available online: <https://sketchfab.com/3d-models/voxel-rat-on-his-tail-1875af655af74355b4f1f647dce444b2> (accessed on 6 June 2021).
30. Chen, B.; Wang, J.; Zhang, J.; Zhang, J.; Chen, S.; Wang, X. The specific absorption rate of tissues in rats exposed to electromagnetic plane waves in the frequency range of 0.05–5 GHz and SARwb in free-moving rats. *Australas. Phys. Eng. Sci. Med.* **2017**, *40*, 21–28. [\[CrossRef\]](#) [\[PubMed\]](#)
31. Shi, J.; Chakarothai, J.; Wang, J.; Fujiwara, O.; Wake, K.; Watanabe, S. Improvement of SAR Accuracy by Combining Two SAR Quantification Methods for Small Animals in Reverberation Chamber Above 10 GHz. *IEEE Access* **2020**, *PP*, 138170–138178. [\[CrossRef\]](#)
32. Yilmaz, T.; Ates Alkan, F. In Vivo Dielectric Properties of Healthy and Benign Rat Mammary Tissues from 500 MHz to 18 GHz. *Sensors* **2020**, *20*, 2214. [\[CrossRef\]](#)
33. Gabriel, S.; Lau, R.W.; Gabriel, C. The dielectric properties of biological tissues: II. Measurements in the frequency range 10 Hz to 20 GHz. *Phys. Med. Biol.* **1996**, *41*, 2251. [\[CrossRef\]](#)

**Disclaimer/Publisher’s Note:** The statements, opinions and data contained in all publications are solely those of the individual author(s) and contributor(s) and not of MDPI and/or the editor(s). MDPI and/or the editor(s) disclaim responsibility for any injury to people or property resulting from any ideas, methods, instructions or products referred to in the content.